Missense models [*Gus*$^{tm(E536A)Sly}$, *Gus*$^{tm(E536Q)Sly}$, and *Gus*$^{tm(L175F)Sly}$] of murine mucopolysaccharidosis type VII produced by targeted mutagenesis

Shunji Tomatsu*†, Koji O. Orii*†, Carole Vogler‡, Jeffrey H. Grubb*, Elizabeth M. Snella*, Monica A. Gutierrez*, Tatiana Dieter*, Kazuko Sukegawa†, Tadao Orii†, Naomi Kondo†, and William S. Sly*§

*Edward A. Doisy Department of Biochemistry and Molecular Biology and ‡Department of Pathology, Saint Louis University School of Medicine, St. Louis, MO 63104; and †Department of Pediatrics, Gifu University School of Medicine, Gifu 500, Japan

Contributed by William S. Sly, September 20, 2002

Human mucopolysaccharidosis VII (MPS VII, Sly syndrome) results from a deficiency of β-glucuronidase (GUS) and has been associated with a wide range in severity of clinical manifestations. To study missense mutant models of murine MPS VII with phenotypes of varying severity, we used targeted mutagenesis to produce E536A and E536Q, corresponding to active-site nucleophile replacements E540A and E540Q in human GUS, and L175F, corresponding to the most common human mutation, L176F. The E536A mouse had no GUS activity in any tissue and displayed a severe phenotype like that of the originally described MPS VII mice carrying a deletion mutation (*gus*$^{mps/mps}$). E536Q and L175F mice had low levels of residual activity and milder phenotypes. All three mutant MPS models showed progressive lysosomal storage in many tissues but had different rates of accumulation. The amount of urinary glycosaminoglycan excretion paralleled the clinical severity, with urinary glycosaminoglycans remarkably higher in E536A mice than in E536Q or L175F mice. Molecular analysis showed that the *Gus* mRNA levels were quantitatively similar in the three mutant mouse strains and normal mice. These mouse models, which mimic different clinical phenotypes of human MPS VII, should be useful in studying pathogenesis and also provide useful models for studying enzyme replacement therapy and targeted correction of missense mutations.

knock-in mice | point mutation | *Cre-loxP*

Mucopolysaccharidosis type VII (MPS VII or Sly syndrome) is a mucopolysaccharide storage disease resulting from a deficiency of β-glucuronidase (GUS, EC 3.2.1.31) (1). In MPS VII, chondroitin sulfate, dermatan sulfate, and heparan sulfate are only partially degraded and accumulate in the lysosomes of many tissues, leading to cellular and organ dysfunction. MPS VII has also been reported in canine, murine, and feline species. Human patients with MPS VII display a wide range of clinical severity, and >45 different mutations have been found in the *GUS* gene (2–13). Around 90% of these are point mutations. L176F accounts for ≈20% of mutant alleles. This mutation was first identified in a Mennonite family (7), and then observed in other populations. Most patients homozygous for L176F have a mild phenotype. This mutation is interesting because cells from L176F patients have <1% of normal GUS activity, but expression of the *L176F* cDNA in COS cells produced nearly as much enzyme activity as the WT control cDNA (7).

Characterization of human GUS protein by x-ray crystallography and homology comparisons among several species suggested R382, E451, and E540 as active-site residues (14). E540 was identified as the active-site nucleophile of the human enzyme (15, 16). Recombinant E540A human GUS had no catalytic activity, but the E540Q GUS showed 0.3% of WT activity (16). One severely affected MPS VII patient with a null mutation at this residue, E540K, has been identified (S.T. and W.S.S., unpublished observation).

The original MPS VII (*gus*$^{mps/mps}$) mice with a 1-bp deletion in exon 10 have morphologic, genetic, and biochemical characteristics similar to those of MPS VII patients (17, 18). The features of this murine model, with a known and uniform genetic constitution, made it attractive for studying experimental therapies for lysosomal storage disorders. Missense mutant mouse models allow functional analysis of specific amino acid replacements. We used targeted mutagenesis to produce three such models of MPS VII: E536A, E536Q, and L175F. The E536 residue in exon 10 was selected because it was implicated as an active-site nucleophile (15, 16). Differences in residual activity between recombinant E536A and E536Q were noted *in vitro* and raised the possibility that the E536Q mutation might provide a milder form of MPS VII than E536A (16). The L175F mutation was selected because the homologous human mutation, L176F, was the most prevalent mutation among MPS VII patients and was usually associated with a mild phenotype.

These mice provided the opportunity to explore (*i*) how the residual enzyme activity level measured *in vitro* correlates with phenotype, (*ii*) how glycosaminoglycan (GAG) storage correlates with the individual mutations, and (*iii*) how phenotypes in mild and severe murine models correlate with those of human patients who have MPS VII caused by similar mutations.

Materials and Methods

Site-Directed Mutagenesis and Targeting Vector Construction. Recombinant phage clones containing the *Gus* locus were isolated from an SvJ129 mouse genomic DNA library (Stratagene). The 5′ 8.5-kb fragment and 3′ 3.9-kb fragment of the murine *Gus* gene (containing exons 1–9 and exon 10, respectively) were subcloned into the pBS vector. The mutations (underlined) were introduced into the appropriate fragments by using the following mutagenic primers: for E536A in exon 10, 5′-CCGATTATCCAGAGCGCGTATGGAGCAGACGCAATC-3′; for E536Q in exon 10, 5′-CCGATTATCCAGAGCCAGTACGGAGCAGACGCAATC-3′; and for L175F in exon 2, 5′-ATCACGATTGCCATTAACAACACATTTACCCCTCATACC-3′. The E536A, E536Q, or L175F point mutation and the indicated additional base changes created new *Bst*UI, *Rsa*I, or *Mse*I restriction sites, respectively. The presence of each point mutation was confirmed by sequence analysis of exons 1–10.

The pPNT-lox vector, generously provided by Shinji Hirotsune (National Human Genome Research Institute, National Institutes of Health, Bethesda), was modified to contain a 3′ phosphoglycerine kinase *neo*^{r} cassette flanked by *loxP* sites and a 5′ thymidine kinase (TK) cassette and was named pPNT-loxP2. The 3′ 3.9-kb *Xho*I–*Not*I fragment of the murine *Gus* gene was introduced at *Not*I/*Xho*I-digested sites of the pPNT-loxP2 vec-

Abbreviations: MPS VII, mucopolysaccharidosis type VII; GAG, glycosaminoglycan; GUS, β-glucuronidase; ES, embryonic stem.

§To whom correspondence should be addressed. E-mail: slyws@slu.edu.

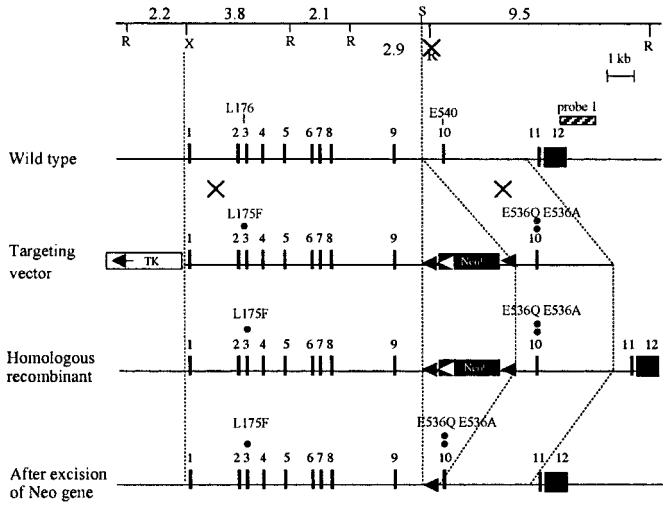

Fig. 1. Targeted mutagenesis of the *Gus* gene. The structure of the endogenous gene, the targeting construct, the homologous recombinant allele, and the neo-excised allele are presented schematically on successive lines. Filled rectangles represent exons and the neomycin resistance gene. The open rectangle indicates the TK gene. The striped bar over the WT allele represents the probe used for Southern blots. Abbreviations for restriction enzymes are: R, *Eco*RI; S, *Sal*I; X, *Xho*I. The R with superimposed X indicates the *Eco*RI site that was destroyed during the construction of the targeting vector by *in vitro* mutagenesis without any effect on the consensus splicing sequences.

tor. Next, the 8.5-kb *Xho*I–*Sal*I fragment containing exons 1–9 was added between the TK and *neo*^{r} genes to create the complete targeting vector. The final construct contained 8.5 and 3.9 kb of 5′ and 3′ homology of the *Gus* gene, respectively, with each point mutation (Fig. 1).

Homologous Recombination in Embryonic Stem (ES) Cells and Generation of Germ-Line Chimeras. The targeting vector (25 μg) was linearized with *Not*I and introduced into the 129/Sv-derived ES cell line RW4 (Incyte Genome Systems, St. Louis; 1×10^7 cells) by electroporation (230 V and 500 μF) in a Bio-Rad gene pulser. After 24 h, the cells were placed under positive/negative selection with 200 μg/ml G418 (GIBCO/BRL) and 2 μM ganciclovir (Syntex Chemicals, Boulder, CO) for 6 days. Colonies resistant to double selection were isolated and analyzed by PCR and Southern blot. The methodology for screening is provided in *Supporting Methods* and Fig. 5, which are published as supporting information on the PNAS web site, www.pnas.org. Two independent, targeted ES clones were injected into C57BL/6J blastocysts, and chimeric males were backcrossed for germ-line transmission to C57BL/6J females. The F_1 mice were crossed with mice expressing *Cre* enzyme to remove the *neo*^{r} gene (19). The resultant neo-excised heterozygous mice were mated to produce homozygous mutant mice. Genotyping was performed by PCR analysis of DNA obtained by tail biopsies at 10 days and confirmed by assaying the GUS activity. The resultant homozygous mice with E536A, E536Q, or L175F point mutations were named $Gus^{tm(E536A)Sly/tm(E536A)Sly}$ [or $Gus^{tm(E536A)Sly}$], $Gus^{tm(E536Q)Sly/tm(E536Q)Sly}$ [or $Gus^{tm(E536Q)Sly}$], and $Gus^{tm(L175F)Sly/tm(L175F)Sly}$ [or $Gus^{tm(L175F)Sly}$], respectively, following the nomenclature recommended by The Jackson Laboratory (www.informatics.jax.org/mgihome/nomen/table.shtml).

Northern Blot Analysis and RT-PCR. Total cellular RNA was isolated from tissues of homozygous MPS VII mutants, heterozygotes, and WT mice by using a guanidinium/phenol solution (RNA-Stat-60, Tel-Test, Friendswood, TX). Twenty micrograms of RNA from each source was denatured in formaldehyde-containing buffer and electrophoresed. The RNA was transferred to nylon membranes (Amersham Pharmacia) and prehybridized at 65°C. Blots were hybridized overnight at 65°C with ^{32}P-labeled mouse *Gus* cDNA probes. mRNA was also analyzed by RT-PCR followed by diagnostic restriction enzyme digestion and analysis on agarose gels (see *Supporting Methods* and Fig. 6, which are published as supporting information on the PNAS web site).

Western Blot Analysis. Tissues were dissected and homogenized immediately (by a Brinkmann Polytron homogenizer for 30 sec at 4°C) in 5 vol of homogenization buffer (25 mM Tris·HCl, pH 7.2/140 mM NaCl/1 mM PMSF). Samples containing 20 μg of protein were analyzed by SDS/PAGE under reducing conditions as described (20). The polypeptides were electronically transferred to Immobilon-P membranes (Millipore). After transblotting, the polypeptides were immunostained by using polyclonal rabbit anti-mouse GUS antibody followed by incubation with goat anti-rabbit IgG (Sigma) coupled with peroxidase. The peroxidase activity was visualized by using a chemiluminescent substrate.

Lysosomal Enzyme Assays. GUS and two other lysosomal enzymes, α-galactosidase and β-hexosaminidase, were assayed fluorometrically by using 4-methylumbelliferyl substrates as described (21–23). Tissues were dissected and homogenized immediately (by a Brinkmann Polytron homogenizer for 30 sec at 4°C) in 5 vol of homogenization buffer (25 mM Tris·HCl, pH 7.2/140 mM NaCl/1 mM PMSF). GUS assays on dilutions of WT tissue extracts were done for 1 h, and on MPS VII [$Gus^{tm(E536A)Sly}$, $Gus^{tm(E536Q)Sly}$, and $Gus^{tm(L175F)Sly}$] extracts for 24 h. Assays of other lysosomal enzymes were incubated for 1 h. Units were nmol hydrolyzed per h, and activity was expressed as units/mg protein, as determined by micro-Lowry assay.

Analysis of GAGs. To determine the μg of GAGs per mg of urinary creatinine, we measured urine with 1,9-dimethylmethylene blue (24–26). Creatinine was measured by mixing 10 μl of a 10-fold diluted urine sample with 50 μl of saturated picric acid (Sigma) and 50 μl of 0.2 M NaOH. Absorbance at 490 nm was read after 20 min and compared with a standard.

Pathology. Multiple tissues from six of each of the MPS VII mouse strains [$Gus^{tm(E536A)Sly}$, $Gus^{tm(E536Q)Sly}$, and $Gus^{tm(L175F)Sly}$], 2–6 months of age, were studied morphologically as described (27). Tissues were evaluated for the extent of lysosomal storage. Alterations in the three strains were compared with each other and with the original MPS VII model ($gus^{mps/mps}$). Long bones from the $Gus^{tm(E536A)Sly}$, $Gus^{tm(E536Q)Sly}$, and $Gus^{tm(L175F)Sly}$ mice were radiographed as described (27).

Results

Generation of $Gus^{tm(E536A)Sly}$, $Gus^{tm(E536Q)Sly}$, and $Gus^{tm(L175F)Sly}$ Knock-In Mice. To introduce each point mutation in the *Gus* gene in mouse ES cells, we designed a targeting vector with a total of 12.4 kb of homologous genomic sequence (Fig. 1). The mutation was cotransferred with *neo* flanked by two *loxP* sites through homologous recombination in ES cells. After selection with G418 and ganciclovir, doubly resistant clones were screened for homologous recombination by PCR followed by Southern blotting with a 3′ external probe. Of 96 clones screened for each mutation by PCR, 20 E536A, 20 E536Q, and 10 L175F were homologous recombinant clones. The presence of the introduced point mutation in the targeted clones was analyzed by PCR amplification followed by restriction enzyme digestion (see *Supporting Methods* and Fig. 6). Thirteen of 20 (65%) clones contained the E536A mutation (*Bst*UI digestion), 14 of 20 (70%) clones contained the E536Q mutation (*Rsa*I digestion), and

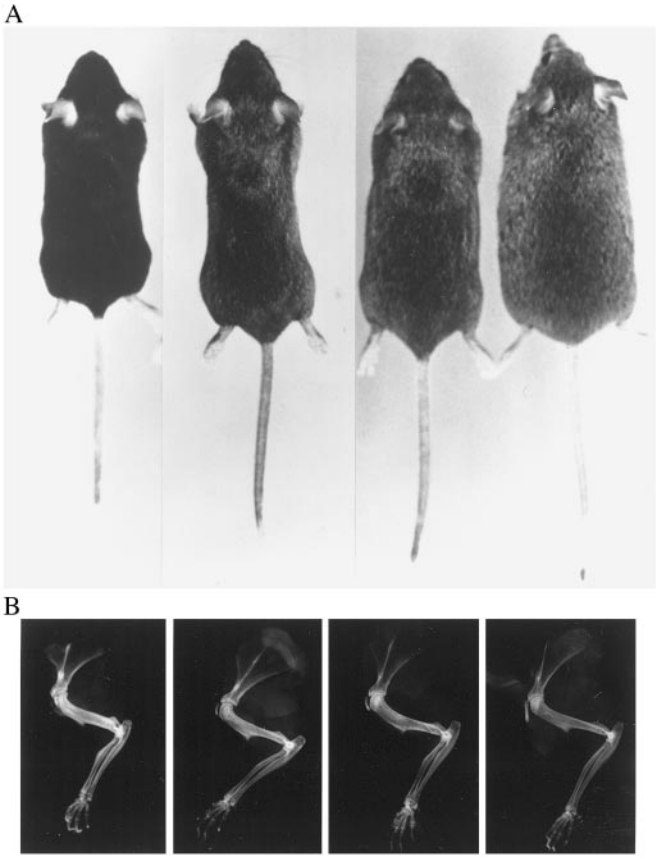

Fig. 2. Morphological and radiographic phenotypes of the *Gus*$^{tm(E536A)Sly}$, *Gus*$^{tm(E536Q)Sly}$, and *Gus*$^{tm(L175F)Sly}$ mice. (*A*) A 6-month-old female *Gus*$^{tm(E536A)Sly}$ mouse (far *Left*) is smaller and has dysmorphic features compared with a normal female mouse (far *Right*) of the same age. Female, 6-month-old *Gus*$^{tm(L175F)Sly}$ (second from *Left*) and *Gus*$^{tm(E536Q)Sly}$ (second from *Right*) mice have milder dysmorphic features compared with *Gus*$^{tm(E536A)Sly}$ mice, although they are easily distinguishable from a normal mouse at this age. The affected mice all have small heads with blunted noses, short limbs, and a hobbled gait, but differ in clinical severity. (*B*) Radiograph of the scapulae and upper extremities of *Gus*$^{tm(E536A)Sly}$ (far *Left*), *Gus*$^{tm(L175F)Sly}$ (second from *Left*), *Gus*$^{tm(E536Q)Sly}$ (second from *Right*), and normal (far *Right*) mice. The long bones of the 6-month-old female *Gus*$^{tm(E536A)Sly}$ mouse (far *Left*) were shortened, broad, and sclerotic compared with the bones of a normal female mouse of the same age (far *Right*). Female *Gus*$^{tm(L175F)Sly}$ (second from *Left*) and *Gus*$^{tm(E536Q)Sly}$ (second from *Right*) mice have similar but milder abnormalities.

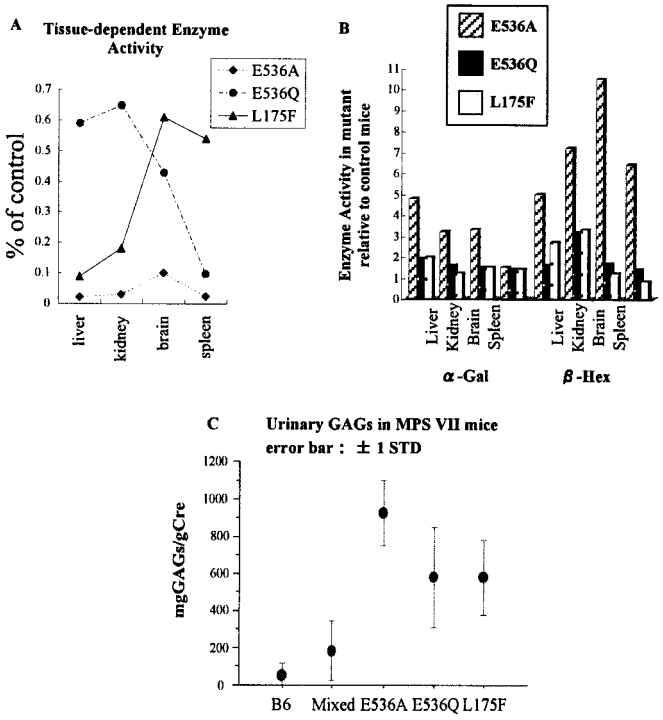

Fig. 3. Tissue levels of enzyme activity and GAGs in *Gus*$^{tm(E536A)Sly}$, *Gus*$^{tm(E536Q)Sly}$, and *Gus*$^{tm(L175F)Sly}$ mice. (*A*) *Gus*$^{tm(E536A)Sly}$ mice have no residual GUS activity in any tissue. *Gus*$^{tm(E536Q)Sly}$ mice have 0.7–0.1% of control level residual activity in liver, kidney, brain, and spleen; *Gus*$^{tm(L175F)Sly}$ mice have <0.2% activity in liver and kidney and 0.5–0.6% in brain and spleen. Control GUS levels were 274, 150, 46, and 520 units/mg in liver, kidney, brain, and spleen, respectively. (*B*) *Gus*$^{tm(E536A)Sly}$ mice show a higher secondary elevation in α-galactosidase (α-gal) and β-hexosaminidase (β-hex) activity compared with *Gus*$^{tm(E536Q)Sly}$ and *Gus*$^{tm(L175F)Sly}$ mice. (*C*) *Gus*$^{tm(E536A)Sly}$, *Gus*$^{tm(E536Q)Sly}$, and *Gus*$^{tm(L175F)Sly}$ mice all have significant elevations in urinary GAGs compared with B6 or mixed background mice. *Gus*$^{tm(E536A)Sly}$ mice have a higher elevation than *Gus*$^{tm(E536Q)Sly}$ and *Gus*$^{tm(L175F)Sly}$ mice.

three of 10 (30%) clones contained the L175F mutation (*Mse*I digestion).

Targeted ES cells containing each mutant allele were injected into C57BL/6J blastocysts, and chimeric males were obtained, followed by germ-line transmission of the mutant allele (F_1). F_1 offspring heterozygous for each of the three mutations were independently intercrossed with C57BL/6J mice to generate F_2 homozygous mice that were 129/Sv × C57BL/6J hybrids. This strategy generated mice heterozygous for the mutation, with the expected Mendelian segregation (WT and mutant, 1:1) at birth.

Phenotype of the MPS VII Missense Mutants. Homozygous E536A MPS VII mice, herein referred to as *Gus*$^{tm(E536A)Sly}$ mice, were not distinguishable phenotypically from heterozygous and homozygous WT littermates at birth but could easily be identified by the time of weaning. They had shortened faces and were slightly smaller. As they aged, their growth retardation, shortened extremities, and facial dysmorphism became more prominent (Fig. 2*A*). The *Gus*$^{tm(L175F)Sly}$ and *Gus*$^{tm(E536Q)Sly}$ mice could not be distinguished from WT mice until at least 3 months of age. Their dysmorphism increased slowly with age, but as adults, it was less severe than that seen in the *Gus*$^{tm(E536A)Sly}$ mice. Fig. 2*A* shows the adult phenotype of the three MPS VII mutant mice and that of a normal WT mouse.

Radiographic analysis of the long bones from *Gus*$^{tm(E536A)Sly}$, *Gus*$^{tm(L175F)Sly}$, and *Gus*$^{tm(E536Q)Sly}$ mice showed skeletal dysplasia similar to that seen in the previously described MPS VII *gus*$^{mps/mps}$ model and in humans with MPS VII. Radiographs comparing the upper extremities of mutant and normal mice are presented in Fig. 2*B*. The long bones were shortened, broad, and sclerotic. The most severe alterations were seen in the *Gus*$^{tm(E536A)Sly}$ mice.

The colonies of *Gus*$^{tm(E536A)Sly}$, *Gus*$^{tm(E536Q)Sly}$, and *Gus*$^{tm(L175F)Sly}$ mice were maintained by brother-sister matings, genotyped by PCR analysis of genomic DNA, and confirmed by enzymatic analysis of extracts of tail samples for GUS activity. Homozygous offspring from these colonies were analyzed for biochemical, morphological, and histopathological phenotypes.

In more than 100 offspring from each mutant line, crosses between heterozygotes produced progeny with a distribution at weaning of 27% +/+, 59% +/−, and 14% −/− for the *Gus*$^{tm(E536A)Sly}$ mice; 26% +/+, 51% +/−, and 23% −/− for the *Gus*$^{tm(E536Q)Sly}$; and 24% +/+, 54% +/−, and 22% −/−

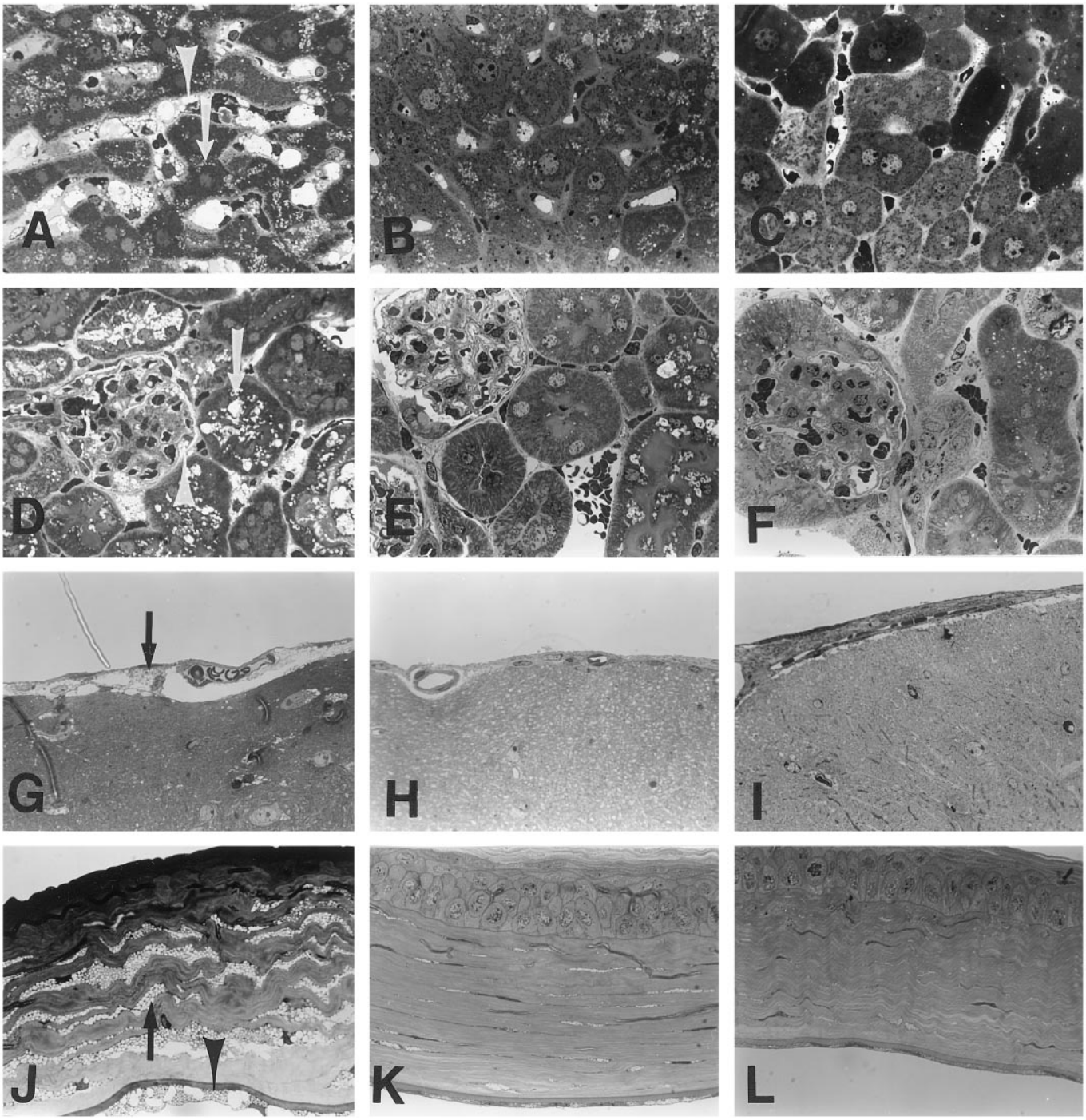

Fig. 4. Histopathology of the *Gus*$^{tm(E536A)Sly}$ (*Left*), *Gus*$^{tm(L175F)Sly}$ (*Center*), and *Gus*$^{tm(E536Q)Sly}$ (*Right*) mice. (*A*) The liver from a 3-month-old *Gus*$^{tm(E536A)Sly}$ mouse has sinus-lining cells (arrowhead) distended by lysosomal storage. Smaller vacuoles affect hepatocytes and pericanalicular distribution (arrow). (*B*) The liver from a 6-month-old *Gus*$^{tm(L175F)Sly}$ mouse has small vacuoles in the Kupffer cells and few vacuoles in the hepatocytes. (*C*) The liver from a 6-month-old *Gus*$^{tm(E536Q)Sly}$ mouse has only small vacuoles in the Kupffer cells. (*D*) Renal tubular epithelial cells (arrow) in the kidney of a 3-month-old *Gus*$^{tm(E536A)Sly}$ mouse contain very large cytoplasmic vacuoles representing lysosomal storage. Glomerular visceral epithelial cells (arrowhead) and interstitial cells also have storage, although their cytoplasmic vacuoles are smaller than those seen in the tubular epithelial cells. *Gus*$^{tm(L175F)Sly}$ (*E*) and *Gus*$^{tm(E536Q)Sly}$ (*F*) mice have very little lysosomal storage in renal tubular epithelial cells and glomerular epithelial cells. (*G*) Vacuolar storage (arrow) is apparent in the meninges overlying the cortex of *Gus*$^{tm(E536A)Sly}$ mice. Meninges of *Gus*$^{tm(L175F)Sly}$ (*H*) and *Gus*$^{tm(E536Q)Sly}$ (*I*) mice show minimal storage. (*J*) The cornea of a 3-month-old *Gus*$^{tm(E536A)Sly}$ mouse is altered with fibrocytes (arrow) and endothelial cells (arrowhead) distended with cytoplasmic vacuolization. Cornea of *Gus*$^{tm(L175F)Sly}$ (*K*) and *Gus*$^{tm(E536Q)Sly}$ (*L*) mice have much less storage in stromal and endothelial cells. (Toluidine blue, 1 cm = 23.8 μm.)

for the *Gus*$^{tm(L175F)Sly}$. Only the *Gus*$^{tm(E536A)Sly}$ offspring have reduced survival in the neonatal period, comparable to that reported in the original MPS VII *gus*$^{mps/mps}$ mice (28).

Biochemical Phenotype of the *Gus*$^{tm(E536A)Sly}$, *Gus*$^{tm(E536Q)Sly}$, and *Gus*$^{tm(L175F)Sly}$ Knock-In Mice. The homozygous *Gus*$^{tm(E536A)Sly}$ mice showed the profound deficiency of GUS reported in the original

MPS VII mice (5) (Fig. 3*A*). Both the *Gus*$^{tm(E536Q)Sly}$ and *Gus*$^{tm(L175F)Sly}$ mice had residual enzyme activity, between 0.1% and 0.7% of normal controls, depending on the tissue measured. The GUS activities in the *Gus*$^{tm(E536Q)Sly}$ and *Gus*$^{tm(L175F)Sly}$ mice were 3- to 30-fold higher than the background levels found in *Gus*$^{tm(E536A)Sly}$ mice. Secondary elevations of other lysosomal enzymes, including α-galactosidase and β-hexosaminidase, were noted in most of the tissues of 3- to 6-month-old mice (Fig. 3*B*). In *Gus*$^{tm(E536A)Sly}$ mice, the α-galactosidase level was 2- to 10-fold higher than that of normal controls. Secondary elevation of α-galactosidase and β-hexosaminidase enzyme activities in tissues tended to increase as the mice aged.

Accumulation of Urinary GAGs. Urine was collected from *Gus*$^{tm(E536A)Sly}$, *Gus*$^{tm(E536Q)Sly}$, *Gus*$^{tm(L175F)Sly}$, and WT mice. The level of GAGs in urine from *Gus*$^{tm(E536A)Sly}$ mice was 10-fold higher than that in normal control mice, whereas the levels from *Gus*$^{tm(E536Q)Sly}$ and *Gus*$^{tm(L175F)Sly}$ mice were increased 3-fold (Fig. 3*C*). There were no overlapping values between those three mutants and the WT mice.

Murine Gus mRNA Transcript and Expression of Murine GUS Protein. Northern blot analyses on total RNA isolated from liver of *Gus*$^{tm(E536A)Sly}$, *Gus*$^{tm(E536Q)Sly}$, *Gus*$^{tm(L175F)Sly}$, and *Gus*$^{+/+}$ littermates showed the presence of a 2.9-kb *Gus* transcript in similar amounts in all mice. Transcripts from *Gus*$^{tm(E536A)Sly}$, *Gus*$^{tm(E536Q)Sly}$, and *Gus*$^{tm(L175F)Sly}$ mice were amplified by RT-PCR and sequenced. Sequencing showed no alterations except the introduced nucleotide alterations. Digestions with *Bst*UI, *Rsa*I, and *Mse*I distinguished the mutant alleles and the normal allele as described (see Fig. 6). Tissues of liver, kidney, spleen, and brain from *Gus*$^{tm(E536A)Sly}$, *Gus*$^{tm(E536Q)Sly}$, *Gus*$^{tm(L175F)Sly}$, and normal control mice were homogenized to analyze the expression of the murine GUS protein. A single band with the expected M_r of the murine GUS protein (75 kDa) was detected by the anti-mouse GUS antibody in multiple tissues of mutant mice (data not shown).

Histopathology of the *Gus*$^{tm(E536A)Sly}$, *Gus*$^{tm(L175F)Sly}$, and *Gus*$^{tm(E536Q)Sly}$ Knock-In Mice. The *Gus*$^{tm(E536A)Sly}$ mice had abundant lysosomal storage in liver, kidney, leptomeningeal cells, and cornea (Fig. 4) and also in spleen, neurons, and retinal pigment epithelium (not shown). The amount and extent of storage was similar to that of the original MPS VII *gus*$^{mps/mps}$ mice (17, 27). In the *Gus*$^{tm(L175F)Sly}$ mice, storage was similar in distribution although less extensive. There was very little storage apparent in the brain and spleen in most of the *Gus*$^{tm(L175F)Sly}$ mice, correlating with the presence of residual GUS activity in these tissues. *Gus*$^{tm(E536Q)Sly}$ mice had much less storage in renal tubular epithelial cells and hepatocytes than the other two strains, which correlated with their higher residual levels of GUS in these two tissues. The bone, articular surface, and synovium of the limb joints also differed in severity of histopathology among the *Gus*$^{tm(E536A)Sly}$, *Gus*$^{tm(L175F)Sly}$, and *Gus*$^{tm(E536Q)Sly}$ mice (see Fig. 7, which is published as supporting information on the PNAS web site).

Discussion

The original *gus*$^{mps/mps}$ MPS VII mouse has a 1-bp deletion in exon 10 and produces only 1/200 of normal levels of *Gus* mRNA (17, 18, 27). These mice have many biochemical, pathological, and phenotypic similarities with MPS VII patients with a severe phenotype. The majority of patients with human MPS VII have different missense mutations that contribute to the broad range of clinical phenotypes. E540 has been identified as the active-site nucleophile of the human *GUS* gene (15, 16). For this reason, we targeted E536 (the residue homologous with E540 in human GUS) to produce a missense mutation conferring a null MPS VII mouse phenotype caused by an enzymatically inactive GUS. The *Gus*$^{tm(E536A)Sly}$ mice exhibit a clinical phenotype characterized by facial dysmorphism, growth retardation, behavioral deficits, systemic bone deformities, and shortened extremities, features very similar to those observed in the original *gus*$^{mps/mps}$ mouse.

The *Gus*$^{tm(L175F)Sly}$ and *Gus*$^{tm(E536Q)Sly}$ mice both show milder clinical phenotypes, detectable residual enzyme activity, less elevation in urinary GAG excretion, and less severe histopathology. In addition, females have the ability to carry a pregnancy to term and produce viable pups, whereas the *Gus*$^{tm(E536A)Sly}$ mice cannot. They also have reduced perinatal mortality compared with the E536A mutant mice. *Gus*$^{tm(E536A)Sly/+}$ $\times$ *Gus*$^{tm(E536A)Sly/+}$ matings produce fewer than the expected 25% $-/-$ mice at weaning. However, the percentage of *Gus*$^{tm(L175F)Sly/tm(L175F)Sly}$ and *Gus*$^{tm(E536Q)Sly/tm(E536Q)Sly}$ mice at weaning did not differ significantly from 25%. Although facial dysmorphism and radiographic features gradually became apparent in the mice homozygous for *Gus*$^{tm(E536Q)Sly}$ and *Gus*$^{tm(L175F)Sly}$ mutations by 4–5 months of age, the mice were larger and appeared healthier during a longer period of their life. The increased viability and fitness of fetuses and newborn pups, the increase in pups surviving to weaning age, and a milder phenotype as adults indicate how much benefit a small amount of residual enzyme can provide.

The lysosomal storage in liver, spleen, and kidney was less in age-matched *Gus*$^{tm(L175F)Sly}$ and *Gus*$^{tm(E536Q)Sly}$ mice than in *Gus*$^{tm(E536A)Sly}$ mice. Quantitative excretion of urinary GAGs was also less than in age-matched *Gus*$^{tm(E536A)Sly}$ mice. Secondary elevation of other lysosomal enzymes was observed in all three mutant strains. However, the lower elevation of α-galactosidase in *Gus*$^{tm(L175F)Sly}$ and *Gus*$^{tm(E536Q)Sly}$ mice than *Gus*$^{tm(E536A)Sly}$ mice shows how sensitive this enzyme is as a secondary marker of GAG accumulation. It is for this reason that α-galactosidase is a valuable marker for following the response to enzyme replacement therapy (29).

We have not identified the mechanism underlying the residual GUS activity produced by the E536Q but not the E536A knock-in allele. *In vitro* expression studies also showed that cells expressing human E540Q (or mouse E536Q) had detectable levels of GUS activity (16). Several factors could explain this residual activity. Glutamate (E) and glutamine (Q) residues are similar amino acids and differ only in one additional amino group on glutamine. The chemical difference, including composition, polarity, and molecular volume, between E and Q is minimal, whereas the chemical difference between E and A (alanine) is greater (30). Possibly, Q has a low level of activity as a nucleophile (16), whereas A has none. Also, enzymatic or nonenzymatic conversion of Q536 to E536 by *in vivo* deamidation could also contribute (31). The higher levels of E536Q activity in liver and kidney compared with other tissues favor this explanation.

The L175F mutation in murine MPS VII led to a milder phenotype, as has been seen with many human MPS VII patients homozygous for the orthologous (L176F) mutation. *In vitro* expression studies showed that overexpression of *GUS* cDNA containing the L176F mutation resulted in 60–80% of the GUS activity of the WT cDNA (7). However, the fibroblasts from human MPS VII patients homozygous for the L176F mutation revealed only 0.5–2% of enzyme activity. The discrepancy between the MPS phenotype, which was consistent with the low level of activity in cells from patients, and the much-higher-than-expected level of GUS activity generated by transient expression has been seen in other mutations of the human *GUS* gene (4, 5). However, the L176F mutation is the most extreme example. It has been suggested that overexpression of mutant monomers could, by mass action, drive the folding reaction or the assembly into tetramers, which achieve a more stable conformation once formed (7). Whether one can

exploit this possibility to test chemical chaperones to drive unstable mutant monomers into stable, active tetramers in mice (or patients) is an interesting therapeutic question (32, 33). The L175F MPS VII mouse allows us to test this hypothesis. In addition, all three of the missense murine models of MPS VII reported here should be useful for developing other strategies for treating lysosomal storage disorders, such as chimeric oligonucleotide-directed gene repair (34).

M. Rafiqul Islam, Yanhua Bi, and Christopher C. Holden provided valuable technical assistance. This work was supported by National Institutes of Health Grants GM34182 and DK40163 (to W.S.S.).

1. Sly, W. S., Quinton, B. A., McAlister, W. H. & Rimoin, D. L. (1973) *J. Pediatr.* **82,** 249–257.
2. Tomatsu, S., Sukegawa, K., Ikedo, Y., Fukuda, S., Yamada, Y., Sasaki, T., Okamoto, H., Kuwabara, T. & Orii, T. (1990) *Gene* **89,** 283–287.
3. Tomatsu, S., Fukuda, S., Sukegawa, K., Ikedo, Y., Yamada, S., Yamada, Y., Sasaki, T., Okamoto, H., Kuwahara, T. & Yamaguchi, S. (1991) *Am. J. Hum. Genet.* **48,** 89–96.
4. Shipley, J. M., Klinkenberg, M., Wu, B. M., Bachinsky, D. R., Grubb, J. H. & Sly, W. S. (1993) *Am. J. Hum. Genet.* **52,** 517–526.
5. Wu, B. M. & Sly, W. S. (1993) *Hum. Mutat.* **2,** 446–457.
6. Vervoort, R., Lissens, W. & Liebaers, I. (1993) *Hum. Mutat.* **2,** 443–445.
7. Wu, B. M., Tomatsu, S., Fukuda, S., Sukegawa, K., Orii, T. & Sly, W. S. (1994) *J. Biol. Chem.* **269,** 23681–23688.
8. Vervoort, R., Islam, M. R., Sly, W. S., Zabot, M. T., Kleijer, W. J., Chabas, A., Fensom, A., Young, E. P., Liebaers, I. & Lissens, W. (1996) *Am. J. Hum. Genet.* **58,** 457–471.
9. Islam, M. R., Vervoort, R., Lissens, W., Hoo, J. J., Valentino, L. A. & Sly, W. S. (1996) *Hum. Genet.* **98,** 281–284.
10. Vervoort, R., Buist, N. R., Kleijer, W. J., Wevers, R., Fryns, J. P., Liebaers, I. & Lissens, W. (1997) *Hum. Genet.* **99,** 462–468.
11. Vervoort, R., Gitzelmann, R., Bosshard, N., Maire, I., Liebaers, I. & Lissens, W. (1998) *Hum. Genet.* **102,** 69–78.
12. Rafiqul, I. M., Gallegos Arreola, M. P., Wong, P., Tomatsu, S., Corona, J. S. & Sly, W. S. (1998) *Prenatal Diagn.* **18,** 822–825.
13. Vervoort, R., Gitzelmann, R., Lissens, W. & Liebaers, I. (1998) *Hum. Genet.* **103,** 686–693.
14. Jain, S., Drendel, W. B., Chen, Z. W., Mathews, F. S., Sly, W. S. & Grubb, J. H. (1996) *Nat. Struct. Biol.* **3,** 375–381.
15. Wong, A. W., He, S., Grubb, J. H., Sly, W. S. & Withers, S. G. (1998) *J. Biol. Chem.* **273,** 34057–34062.
16. Islam, M. R., Tomatsu, S., Shah, G. N., Grubb, J. H., Jain, S. & Sly, W. S. (1999) *J. Biol. Chem.* **274,** 23451–23455.
17. Birkenmeier, E. H., Davisson, M. T., Beamer, W. G., Ganschow, R. E., Vogler, C. A., Gwynn, B., Lyford, K. A., Maltais, L. M. & Wawrzyniak, C. J. (1989) *J. Clin. Invest.* **83,** 1258–1266.
18. Sands, M. S. & Birkenmeier, E. H. (1993) *Proc. Natl. Acad. Sci. USA* **90,** 6567–6571.
19. Marth, J. D. (1996) *J. Clin. Invest.* **97,** 1999–2002.
20. Laemmli, U. K. (1970) *Nature* **227,** 680–685.
21. Wagner, T. E., Hoppe, P. C., Jollick, J. D., Scholl, D. R., Hodinka, R. L. & Gault, J. B. (1981) *Proc. Natl. Acad. Sci. USA* **78,** 6376–6380.
22. Glaser, J. H. & Sly, W. S. (1973) *J. Lab. Clin. Med.* **82,** 969–977.
23. Peterson, G. L. (1979) *Anal. Biochem.* **100,** 201–220.
24. Bjornsson, S. (1993) *Anal. Biochem.* **210,** 282–291.
25. Whitley, C. B., Ridnour, M. D., Draper, K. A., Dutton, C. M. & Neglia, J. P. (1989) *Clin. Chem.* **35,** 374–379.
26. Poorthuis, B. J., Romme, A. E., Willemsen, R. & Wagemaker, G. (1994) *Pediatr. Res.* **36,** 187–193.
27. Vogler, C., Birkenmeier, E. H., Sly, W. S., Levy, B., Pegors, C., Kyle, J. W. & Beamer, W. G. (1990) *Am. J. Pathol.* **136,** 207–217.
28. Soper, B. W., Pung, A. W., Vogler, C. A., Grubb, J. H., Sly, W. S. & Barker, J. E. (1999) *Pediatr. Res.* **45,** 180–186.
29. Sands, M. S., Vogler, C., Kyle, J. W., Grubb, J. H., Levy, B., Galvin, N., Sly, W. S. & Birkenmeier, E. H. (1994) *J. Clin. Invest.* **93,** 2324–2331.
30. Grantham, R. (1974) *Science* **185,** 862–864.
31. Robinson, N. E. & Robinson, A. B. (2001) *Proc. Natl. Acad. Sci. USA* **98,** 12409–12413.
32. Tamarappoo, B. K. & Verkman, A. S. (1998) *J. Clin. Invest.* **101,** 2257–2267.
33. Frustaci, A., Chimenti, C., Ricci, R., Natale, L., Russo, M. A., Pieroni, M., Eng, C. M. & Desnick, R. J. (2001) *N. Engl. J. Med.* **345,** 25–32.
34. Kren, B. T., Bandyopadhyay, P. & Steer, C. J. (1998) *Nat. Med.* **4,** 285–290.